UCRL-JC-133956

PCMDI Report No. 52

SAMPLING STRATEGIES FOR THE COMPARISON OF CLIMATE MODEL CALCULATED AND SATELLITE OBSERVED BRIGHTNESS TEMPERATURES

By

Richard J. Engelen and Laura D. Fowler
Dept. of Atmospheric Science, Colorado State University
Fort Collins, Colorado

Peter J. Gleckler and Michael F. Wehner
Program for Climate Model Diagnosis and Intercomparison, Lawrence Livermore National Laboratory, Livermore, California

May 1999

PROGRAM FOR CLIMATE MODEL DIAGNOSIS AND INTERCOMPARISON
UNIVERSITY OF CALIFORNIA, LAWRENCE LIVERMORE NATIONAL LABORATORY, LIVERMORE, CA 94550

Sampling Strategies for the Comparison of Climate Model Calculated and Satellite Observed Brightness Temperatures

Richard J. Engelen and Laura D. Fowler
Dept. of Atmospheric Science, Colorado State University, Fort Collins, Colorado

Peter J. Gleckler and Michael F. Wehner
Program for Climate Model Diagnosis and Intercomparison, Lawrence Livermore National Laboratory, Livermore, California

May 1999

Abstract

Brightness temperatures derived from polar orbiting satellites are valuable for the evaluation of global climate models. However, the effect of orbital constraints must be accounted to ensure valid comparisons. As part of the AMIP II climate model comparisons, this study seeks to evaluate the bias of possible model output sampling strategies, and whether they can be practically implemented to provide meaningful comparisons with these satellite observations. We compare various sampling strategies with a proxy satellite data set constructed from model output and actual TOVS orbital trajectories, rather than with the observations themselves. To a large extent, this enables isolation of the sampling error from biases caused by deficiencies in the modeled climate processes. Our results suggest that the traditional method of calculating brightness temperatures from monthly mean temperature and moisture profiles yields biases from both nonlinear effects and the removal of the diurnal cycle, that may be unacceptable in many applications. However, our results also suggest that a brightness temperature calculation every six hours of the simulation provides substantially lower sampling biases provided that there are two or more properly aligned satellites. This is encouraging because it means for many applications modelers need not accurately mimic actual satellite trajectories in the sampling of their simulations. However, if only one satellite is available for comparison with simulations, more sophisticated sampling seems necessary. For such circumstances, we introduce a simple procedure that serves as a useful approximation to the rather complex procedure required to sample a model exactly as a polar orbiting satellite does the Earth.

1. Introduction

Satellite observations play an increasingly important role in climate research. Due to their daily global coverage they offer potential for detecting climate trends and for the comparison with general circulation models (GCMs) [e.g., Christy (1998), Fowler (1996), Hack (1998), Rotstayn (1998)]. Relatively long data records of the Earth radiation budget (ERB), atmospheric temperatures, water vapor and cloud observations (among others) continue to be compiled for these purposes [e.g., Barkstrom (1984), Randel (1996), Schiffer (1983)].

As part of the ongoing Atmospheric Model Intercomparison Project (AMIP) (http://www-pcmdi.llnl.gov/amip/), an experimental subproject has been proposed that aims to compare monthly mean brightness temperatures calculated from GCMs with Tiros Operational Vertical Sounder (TOVS) observed brightness temperatures for the period 1979 to 1996. A selection of infrared and microwave channels (sensitive to surface temperature, atmospheric temperature and water vapor concentrations) will be simulated in the models. This represents a new and important approach that compares climate models with satellite observations in a direct way.

Unlike satellite-derived ERB and cloud climatologies that were designed to be used to assess the performance of climate models to simulate top-of-the-atmosphere radiation and clouds, the 17-year record of TOVS brightness temperatures is not well suited for direct comparison against monthly mean brightness temperatures simulated in large-scale models. In order to objectively compare simulated against satellite-derived brightness temperatures, the outstanding issue that needs to be addressed is the impact of the asynoptic sampling (i.e., not every point on Earth is sampled at the same time) of the NOAA-series satellites on the computation of the monthly mean observed brightness temperatures. Polar orbiting satellites, as the NOAA-series satellites, observe each point on Earth twice a day at the same local time every day, leading to an undersampling of atmospheric parameters and systematic biases in the computation of their monthly means, as discussed by Salby (1989) and Salby (1997). Due to this undersampling of the diurnal cycle, the satellite observations from polar-orbiting platforms do not provide "true" monthly means, especially for atmospheric parameters that have a large non-symmetric diurnal cycle.

Recently, some studies also addressed the inhomogeneity of satellite derived Outgoing Longwave Radiation (OLR) data sets due to the change of local overpass times between the individual satellites. Gadgil (1992) were among the first to attribute the difference in amplitude between NOAA-SR and NOAA-7 observed OLR to the difference in local overpass time of the two satellites. Kayano (1995) used empirical orthogonal function analysis to correct the OLR data set for the above mentioned problem. Waliser (1997) improved the empirical orthogonal function method to also account for the drift of the various satellites.

For our AMIP study, the satellites are the ground-truth to which we would like to compare results from the GCMs. Therefore, a sampling strategy is needed in order to minimize biases in the comparison of model calculated brightness temperatures with satellite observations, especially, because we do not intend to run diurnal models through

our satellite data as was for instance done for the ERB and cloud climatologies [Brooks (1986), Young (1998)]. Because most of the time the TOVS Pathfinder Radiance data set consists of observations from 2 satellites, we will primarily focus on sampling biases when using 4 observations per day. However, for completeness we will also consider sampling biases caused by the use of only one satellite.

In this study we evaluate a variety of sampling strategies applied to GCMs with the objective of determining which is most suitable for comparison with monthly average brightness temperatures derived from polar orbiting satellites. The differences in monthly mean brightness temperatures for some specific TOVS infrared and microwave channels due to those different sampling strategies are presented. The aim is to understand the character of biases introduced by the satellite sampling and to adjust the sampling of the GCMs to minimize these biases in order to make valid comparisons with satellite observations.

Our approach is to construct a proxy for the satellite data set using model output. We then sample this proxy data with a variety of methods and compare their differences. Using this approach, differences isolate the effects of the sampling strategy, not model deficiencies that one would encounter when comparing with actual satellite data.

2. Models and observations

The sampling experiments are performed for two different climate models, the Colorado State University (CSU) GCM [Ding (1998), Fowler (1996), Pan (1998)] and the Lawrence Livermore National Laboratory (LLNL) GCM [Wehner (1995)a, Wehner (1995)b]. The CSU model has a 4x5-degree horizontal latitude-longitude grid and 17 vertical modified sigma levels between the surface and 51.3 hPa. The LLNL model has a 4x5-degree horizontal latitude-longitude grid and 15 vertical modified sigma levels between the surface and 1 hPa. Two GCMs are used in this study, because the magnitude of the errors due to different sampling strategies is dependent on the simulated diurnal cycles. The LLNL model provided 1-hourly output of temperature profiles, water vapor profiles, and calculated brightness temperatures for a non-specific January month. The different sampling strategies were then performed outside the model. The CSU model performed the sampling strategies inside the model.

In both GCMs a Malkmus broad band radiation code [Engelen (1999)] was used to calculate brightness temperatures from the model simulated temperature and water vapor profiles. This radiative transfer model calculates band averaged brightness temperatures for the various TOVS infrared and microwave channels, where the respective instrument response functions are incorporated in the model. Brightness temperatures for 6 High resolution Infrared Radiation Sounder (TOVS/HIRS) channels and 4 Microwave Sounding Unit (TOVS/MSU) channels were simulated using temperature, carbon dioxide, and water vapor profiles from the GCMs. Where clouds are present, the cloud absorption was not taken into account. The effects of clouds here are extracted much in the same way as in the now traditional "Method II" clear-sky radiative flux calculations [Cess (1987)]. Table 1 provides a description of the 10 channels.

The TOVS data set is available since the launch of the first NOAA-series satellite in late 1978 until present. This intersects nicely with the integration period of AMIP II

simulations, which start at 00Z on January 1 1979 and end at 00 Z on March 1 1996. A 17-year record of monthly-mean simulated brightness temperatures at six infrared and four microwave channels available on the TOVS/HIRS and TOVS/MSU instruments can therefore be compared with observations. Table 1 provides characteristics of these sounding channels. The HIRS channel 8 and MSU channel 1 (later referred to as HIRS8 and MSU1, respectively) are both sensitive to the surface temperatures. The HIRS channels 4 and 6 and MSU channels 2 and 3 are sensitive to tropospheric temperatures averaged over broad layers. The HIRS channels 10, 11, and 12 are sensitive to both tropospheric temperatures and water vapor concentrations. Finally, MSU channel 4 is sensitive to upper-tropospheric temperatures. Noise levels are given in degrees Kelvin and include contributions from pre-processing and cloud-clearing as well as radiometric noise [Eyre (1987)].

On a normal basis, brightness temperatures are available four times per day from two NOAA sun-synchronous satellites, one in a morning/evening orbit and the other in an afternoon/night orbit with the aim to capture the diurnal cycle of
temperature and water vapor. Brightness temperatures are only retrieved from clear and clear-cloudy (up to 75 % partial cloud cover) radiances. This yields a greater uncertainty in the retrieval of monthly mean brightness temperatures over convectively active regions in the tropics and the middle latitude storm tracks, relative to that of monthly mean brightness temperatures measured over desert regions and the clear-sky subtropical oceans.

Several problems need to be addressed when using TOVS data to study temperature trends [Trenberth (1992), Hurrell (1998), Christy (1998)] or to assess model performance. For example, temporal inhomogeneities due to changes in the instruments, changes in equatorial crossing times between the successive satellites at the initial launch and drift in the satellite orbits with time, and changes in the algorithms used to convert radiances to brightness temperatures. Another difficulty in using TOVS data is a large number of gaps in the times series that can range from several hours to over a month due to instrument failures and problems occurring during the operational processing of the data, as discussed in Wu (1993) and Bates (1996). Finally, there were times during which data from only one satellite was available resulting in
monthly mean retrieved brightness temperatures based on two samples per day. Efforts to reduce systematic biases due to intercalibration between instruments have been discussed by Wu (1993) and Bates (1996) while methods to
remove satellite equatorial crossing time biases have been proposed by Waliser (1997). Once these biases are removed, the two outstanding questions that remain to be answered are:

1) How to account for the asynoptic sampling of the satellite when comparing simulated versus satellite derived brightness
temperatures?

2) How to account for the undersampling of the satellite over overcast regions?

3. Sampling strategies

The primary objective of this study is to determine how best to sample climate model output for comparison with available polar-orbiting satellite observations.

Several issues influence our approach. The first relates to the imperfections of the observations. Monthly mean brightness temperatures from TOVS are inherently biased because of the asynoptic sampling. On the other hand, there are no sampling biases with a GCM if it is sampled at every simulated time step. While generally it is desirable to minimize biases, for our purposes it may be preferable to bias the model output in a manner that is consistent with biased satellite data. One of the objectives of this study is to consider if we should intentionally bias the model output for optimal comparison with observations.

A second issue of concern to us is practicality. How often must we run our radiation code to adequately capture the true monthly averaged brightness temperatures of the model? Although it represents exactness of the simulation, one would like to avoid having to run a diagnostic radiation code at every simulated time step and grid point if possible. Additionally, models are generally set up to sample every location of the globe at the same instant, which is very different from the sampling of a polar orbiting satellite. Thus in our investigation we are considering not just the accuracy of our results, but how much model-specific effort (computational and code development) is required to obtain these results. Table 2 identifies the sampling strategies that we have considered for computing monthly average brightness temperatures for our GCM simulations. The first three approximate the asynoptic sampling of polar orbiting satellites, while the last three are more typical approaches used in GCMs, with each grid point being sampled at the same instant.

With EXACTSAT the model is sampled (i.e., the diagnostic radiation code is run) only in those grid boxes where we have TOVS observations. This means that samples are taken only in clear sky and cloud-cleared (based on those observed) conditions. The light-grey grid boxes in Figure 1 represent an example of the EXACTSAT calculation. A disadvantage to this calculation is that at any given time the clouds observed are in general different from those simulated, and thus there is another class of sampling bias inherent in the "exact" sampling case. IDEALSAT is similar to EXACTSAT in that the actual path of the satellite orbit is also simulated. The difference with EXACTSOL is that computation of the brightness temperatures is being done for every grid-box seen by the satellite, even when the satellite-derived clear-sky brightness temperature is not available due to observed cloudy conditions. In Figure 1, the dark grey boxes are boxes for which TOVS brightness temperatures were missing but for which brightness temperatures were computed, in addition to those computed over the light grey boxes. Adding the light and dark grey boxes reproduces the path of the satellite simulated in each GCM. The difference between IDEALSAT and EXACSAT will provide an estimate of the error in the monthly mean calculation of brightness temperatures due to the undersampling of the satellite over overcast regions. LOCALSOL represents an approximation to the satellite sampling, with each grid point being sampled at the same local time(s) each day. The ascending and descending branches of each orbit are approximated as north-south oriented bands centered over the longitude of the equatorial crossing time of each orbit. This approximation is represented in Figure 2 with the black vertical bars, the width of which is approximately the same as the satellite swath. LOCALSOL is considered because its simplification to EXACTSAT may be appealing to modelers if it proves to be a sufficient approximation.

The remaining three sampling strategies on Table 2 are commonly used in GCMs. EXACTMOD is generally used to average physical process fields such as precipitation and radiative fluxes, and basically amounts to including every
simulated time step in the averaging process. GMT averaging (usually sampling at every grid point at 0, 6, 12 and 18Z) is used as an approximation to EXACTMOD for more smoothly varying fields such as temperature and winds. Since here we are dealing with radiation calculations where diurnal variations may be important, we suspect that GMT may not be a good approximation of EXACTMOD for
some of the channels in Table 1. MONTHAVG is the most extreme and common approximation [e.g., Mo (1995), Basist (1997)], for studies involving diagnostic radiation calculations. Here, the radiation code is only run once (per grid box), on the monthly averages of the simulated temperature and humidity profiles. The fact that this method is commonly used but likely to include important biases is another motivation for this study.

In the next section we will systematically compare these approximations, in search of the most practical means of sampling GCMs for comparison with polar orbiting satellites.

4. Sampling error in monthly mean brightness temperatures

The EXACSAT experiment will be used as our "control" against which the other sampling experiments are compared, since EXACTSAT simulates most faithfully the actual samplings of the NOAA-series satellites, but at the temporal and spatial resolutions of the LLNL and CSU GCMs. To produce monthly averaged brightness temperatures with EXACTSAT, IDEALSAT and LOCALSOL, we simulated the actual or idealized paths of the NOAA-10 and NOAA-11 satellites, both separately and then combined. By comparing the results obtained using one and two satellites, we can infer the effect of poorly sampling the diurnal cycle of surface temperature, atmospheric temperature, and water vapor on the global distributions of monthly averaged brightness temperatures. At launch date, the ascending and descending nodes of NOAA-10 were set to 7:30am/pm (morning satellite) whereas those of NOAA-11 were set to 1:30am/pm (afternoon satellite), respectively. Our analysis of biases in the brightness temperatures focuses on the HIRS channels 8 and 12 (later referred to as HIRS8 and HIRS12), which are sensitive to the surface and the mid- to upper troposphere, respectively. Tables 3, 4, and 5 summarize the root-mean-square HIRS8 and HIRS12 brightness temperature differences for the LLNL and CSU GCMs, respectively. These are area-weighted root-mean-square differences between the brightness temperature fields using the different sampling strategies.

To help understand the differences presented later in this section, monthly averaged distributions of HIRS8 and HIRS12 brightness temperatures computed with the CSU model (running our radiation code) with the EXACTSAT sampling are shown in Figures 2 and 3.

The geographical distribution of the HIRS8 brightness temperature strongly resembles the surface temperature simulated by the GCM (not shown here for brevity). This is not surprising since atmospheric absorption in channel 8 is weak, so channel 8 is mostly sensitive to the surface temperature. As for the surface temperature, the HIRS8

brightness temperature decreases rapidly poleward, especially over land in the winter hemisphere. Its distribution and magnitude are relatively constant between 30N and 30S, especially over oceans, since during the simulations the sea surface temperature was held to constant January mean climatological values. The water vapor absorption in channel 12 is strong and therefore the HIRS12 brightness temperatures resemble the emission by water vapor in the mid- and upper troposphere, very similar to that of the top-of-the-atmosphere outgoing longwave radiation (not shown here, for brevity). Similar to the outgoing longwave radiation, the HIRS12 brightness temperatures rapidly decrease with increasing latitudes. In the tropics, high brightness temperatures are observed over areas with low upper tropospheric humidities, and relative low brightness temperatures over areas with high upper tropospheric humidities.

To understand the chief differences between EXACTSAT and the other sampling methods, it is important to understand the impact of the different equatorial crossing times of NOAA-10 and NOAA-11 on their sampling. Figures 4 and 5 show the geographical distributions of the fractional decrease in the number of satellite samples between IDEALSAT and EXACTSAT, accumulated over January for NOAA-10 and NOAA-11 separately. The fractional decrease (rather than absolute) between IDEALSAT and EXACTSAT was chosen to account for the fact that the number of observations increases with latitude due to a larger overlap of the satellite orbits. For a given grid cell, the number of satellite samples in EXACTSAT is defined as the number of occasions it is defined as clear-sky or cloud-cleared by the satellite retrieval algorithm. In general, the decrease in the number of satellite samples is smaller for NOAA-10 than NOAA-11, indicating that NOAA-11 passes over areas at local times when cloudiness is more extensively developed than when seen by NOAA-10, especially over land. Over the tropical convective regions, as the Amazon Basin, Southern Africa, and the South-East Asian monsoon in January, this result makes sense since deep convection develops early- and mid-afternoon, or closer to the 1:30 pm equatorial crossing time of NOAA-11 than the 19:30 pm equatorial crossing time of NOAA-12. Over desert regions such as the Sahara desert, NOAA-11 has many cloudy scenes, especially around the 1.30 pm overpass. This is most probably caused by the cloud detection algorithm. One condition that defines a scene as cloudy is an albedo greater than 0.3 over land [McMillin (1982)]. Over deserts this is quite often the case. A very bright surface is therefore mistakenly seen as a cloud.

In EXACTSAT, the number of times an individual grid-box is sampled per month depends on whether or not the satellite scene of view was defined as clear or clear-cloudy, and a TOVS temperature was actually retrieved for that specific grid-box. This yields simulated brightness temperatures to be computed over grid-boxes that are seen as cloud-free from satellites but are actually cloudy in models. One way to avoid using cloudy atmospheric profiles to compute clear-sky brightness temperatures would be to adopt Method I of Cess (1987), and only compute brightness temperatures for grid-boxes with cloud fractions equal to zero. Tests demonstrate that this would greatly reduce the number of times brightness temperatures that are calculated over mostly cloudy regions, and would also strongly differ from the satellite sampling itself. Instead, we choose to sample all grid boxes that are observed by the satellite, regardless of the cloud fraction, following Cess and Potter's Method II.

In the GCM brightness temperature comparisons we are mainly interested in monthly means, because we do not expect day-to-day agreement between the simulations and the satellite observations. Therefore, it seems obvious to simply calculate brightness temperatures from monthly mean model output and compare these to monthly averaged satellite observed brightness temperatures. However, because satellites sample asynoptically and because radiative transfer can be highly non-linear, this simple approximation is expected to introduce errors. Figures 6 and 7 show the difference between monthly averaged brightness temperatures calculated from satellite sampled profiles (EXACTSAT) using both NOAA 10 and NOAA 11 and brightness temperatures calculated from monthly mean temperature and water vapor profiles (MONTHAVG) for TOVS/HIRS simulated channels 8 and 12. For channel 8, differences occur mainly over land and can be as large as 3K. Over the ocean the differences are negligible. For channel 12 the differences are not related to the land/ocean distribution, but to the water vapor distribution. Differences are as large as 1.5K in the tropics and more than 2.5K at higher latitudes. Positive biases are observed in the tropics where the atmosphere contains much water vapor; negative biases are observed at high latitudes where the atmosphere is generally very dry.

From Figures 6 and 7 it seems reasonable to assume that the biases for channel 8 are mainly caused by the inability of the satellite sampling to capture the large diurnal cycle of the surface temperature over land and the biases for channel 12 are mainly caused by the non-linearity of the radiative transfer. Figures 8 and 9 further illustrate this. If the non-linearity is causing the biases, different biases for EXACTSAT - MONTHAVG and EXACTSAT - EXACTMOD are expected, which is the case for channel 12. On the other hand, if the satellite sampling is causing the biases, the biases for EXACTSAT - MONTHAVG and EXACTSAT - EXACTMOD should be about the same, which is the case for channel 8. This simple analysis demonstrates the importance of calculating brightness temperatures at higher temporal frequency than monthly. Because channel 8 is affected most by the asynoptic sampling of the satellites, we will consider this channel into more detail.

The asynoptic satellite sampling using 2 polar orbiting satellites is limited to 4 observations per grid box per day. Therefore, as a first attempt to approximate this asynoptic sampling, we used the GMT sampling, i.e., sample each gridbox at 0, 6, 12, and 18 GMT. This sampling method is widely used in climate studies and easy to implement. Figures 10 and 11 show the difference between monthly averaged brightness temperatures using the EXACTSAT sampling and the GMT sampling for January and July, respectively. A first conclusion from these figures is that the GMT sampling strategy did not improve significantly on the EXACTMOD sampling. Also, the sampling biases show a seasonal dependence. Although the (sub)tropical biases are almost the same for January and July, biases in the northern hemispheric mid- and high latitudes are much larger in July than in January.

The results above indicate that using a sampling method that is not close to the actual satellite sampling generates significant biases in the monthly mean brightness temperature fields that make it harder to interpret results from the comparison between the GCMs and the actual satellite observations. However, the implementation of the exact satellite sampling in a GCM is an arduous task. In order to simplify the exact sampling of the satellite, the asynoptic sampling can be approximated by a so-called local time

sampling (see Section 3). For each hour of the model run, this method samples a latitude band that has the same local time as the satellite equatorial overpass and approximately the width of the satellite swath. Figure 1 shows an example of this local time sampling.

As with the others, there are drawbacks to this sampling method. First, because the satellite is flying over the poles from day to night, the local time approximation gets worse at higher latitudes. Second, some of the polar orbiting satellites are drifting over the years, which means that the local time of their overpass is changing. Third, because we only have useful brightness temperatures over regions where the sky is clear or where cloud-clearing is possible, regions with extensive cloud cover are oversampled by the LOCALSOL sampling relative to the EXACTSAT sampling. Figures 12 and 13 show the difference in monthly mean brightness temperature between the EXACTSAT sampling and local time sampling (LOCALSOL). Because only one month is considered here, drifting of the satellite does not play a role. Although the sampling biases in the (sub)tropics are reduced compared to the GMT sampling, biases at higher latitudes remain large, especially in summer. Apparently, the LOCALSOL sampling of the diurnal cycle is close enough to the EXACTSAT sampling in the tropics, but deviates significantly at higher latitudes. Furthermore, there is still a sampling problem over convective regions and deserts. We will consider the latter problem first and then get back to the high-latitude sampling problem.

Figures 4 and 5 showed that clouds have a significant effect on the satellite sampling. The satellites only provide useful observations over clear regions and regions where cloud-clearing [McMillin (1982)] is possible. To investigate this effect we compared the EXACTSAT sampling with the IDEALSAT sampling. EXACTSAT imposes the clouds as observed by satellite without regard to the simulated cloud extent. IDEALSAT samples all grid boxes that are observed by the satellite regardless of observed or simulated cloud cover. However, such inconsistencies appear to be unavoidable with any sampling technique.

Figures 14 and 15 show the difference in monthly mean brightness temperature between these two sampling methods for January and July, respectively. The differences in these comparisons are solely caused by the effect of cloud cover as retrieved from the satellite cloud detection algorithm. It is quite interesting to see that clouds seem to account for most of the differences between the EXACTSAT sampling and the other sampling methods. The difference in the HIRS8 brightness temperature between EXACTSAT and IDEALSAT is positive over the Amazon Basin and Southern Africa, as well as over the winter monsoon of South East Asia. This difference is negative over a major part of the Sahara desert and the Australian desert, as well as above areas of high sea-level pressure in the winter hemisphere, across the Northern American and Asian continents. Over tropical convective activity regions, the decrease in the HIRS8 brightness temperatures between EXACTSAT and IDEALSAT results because 1) the number of samplings is greater in IDEALSAT than in EXACTSAT, and 2) the surface temperature is systematically cooler than it would be under clear-sky conditions due to the development of extended anvils at the tops of convective towers. The persistent shadowing impact of extended cloudiness developing around the equatorial crossing time of the NOAA-11 satellite is the factor that probably influences the most the difference in the HIRS8 brightness temperature between the EXACTSAT and IDEALSAT experiments. Over desert regions, the increase in the HIRS8 brightness temperatures

between EXACTSAT and IDEALSAT results, as over tropical convective activity regions, because of the increased number of satellite overpasses between EXACTSAT and IDEALSAT. This increased number of satellite overpasses per grid box results because in EXACTSAT many NOAA-11 observations are erroneously flagged as cloudy, biasing the average temperatures to cooler morning and evening temperatures. The increase in the HIRS8 brightness temperatures over areas of high sea-level pressure over land results because of decreased cloudiness, allowing IDEALSAT to compute brightness temperatures using surface temperatures that are strongly influenced by the simulated cloud fraction. Apparently, the afternoon observations of NOAA-11 have a strong effect on the calculated average brightness temperatures. The lesser effect of the NOAA-10 temporal sampling on the HIRS8 brightness temperature differences between EXACTSAT and IDEALSAT is clearly seen when looking at the rms differences for January given in Tables 3 and 5. For the LLNL GCM, the HIRS8 rms difference is equal to 0.57 K for NOAA-10 and equal to 2.09 K for NOAA-11. For the CSU GCM, the HIRS8 rms difference increases from 0.39 K for NOAA-10 to 1.12 K for NOAA-11. Our analysis leads us to conclude that differences in cloud regimes, mainly the difference in the frequency of occurrence of clouds between the tropics and the extratropics, are mostly responsible for the regional variations in the HIRS8 brightness temperature differences between the EXACSAT and IDEALSAT experiments. Over deserts the main effect is the erroneous cloud detection, especially in the NOAA-11 observations

We now return to the high latitude sampling problem. Most differences between EXACTSAT and the other sampling methods can be explained in terms of clouds, but an interesting feature appears over high northern latitudes in July. Although differences between EXACTSAT and the model samplings (EXACTMOD, GMT, and LOCALSOL) are quite large (up to 2.5K), differences between EXACTSAT and IDEALSAT for these regions are small (less than 1K). After looking into more detail to this phenomenon, we found that it is caused by the fact that the satellite overpasses are no longer equally spaced in time. At high latitudes the approximate overpass times are 2, 8, 12, and 18 hour local time. Therefore, during the long high-latitude summer days the satellite samples 3 times during the day and only 1 time during the night. The average is thus biased to higher daytime temperatures. In winter this effect does not exist, because the days are much shorter.

For HIRS12 the sampling problems described above have a much smaller magnitude as can be seen in Tables 3, 4, and 5. The rms differences are small and approximately the same for all comparisons apart from the MONTHAVG sampling. The main issue for this channel is therefore the non-linear character of the radiative transfer.

Two satellites are not always available, and it is therefore interesting to look at the effect of having only one polar orbiting platform, which provides 2 samples per day for a given location. Figure 16 shows the difference in monthly mean channel 8 brightness temperatures between the EXACTSAT sampling for NOAA 10 and the GMT sampling. Comparing this figure with Figure 6, we see that the bias is greatly enhanced. Largest values can be seen over Africa with amplitudes up to 7K with biases up to 5K over the other continents. Comparing EXACTSAT with GMT for NOAA 10 shows almost the same differences as seen in Figure 17. However, when we use our LOCALSOL approximation in this one-satellite case, differences are much reduced as can be seen in

Figure 18. Differences are again in the order of 1 to 2K and only slightly larger than the differences of EXACTSAT - IDEALSAT, which are presented in Figure 19.

These last comparisons stress the importance of simultaneously having multiple polar orbiting platforms with different equatorial crossing times. Unfortunately, there are some periods in the TOVS data set where there was only one operational platform available.

5. Conclusions

When comparing brightness temperatures computed from GCM simulations with those derived from observations, it is important to properly address the impact of the asynoptic satellite sampling versus synoptic GCM sampling on the computation of monthly means.

The TOVS brightness temperature data set suffers from 2 distinct problems that need to be corrected in order to make good comparisons with the GCMs. First, the various polar orbiting NOAA satellites have been drifting away from their original inserted orbit. This drift causes a gradual change in equatorial crossing times and thus in local overpass time during the lifetime of the satellite. A sharp change in local overpass time occurs when a satellite is replaced by a new one. Waliser (1997), among others, showed recently that this sampling problem can be corrected with an empirical orthogonal function method. This drifting problem and its correction are especially important when we look at trends in the brightness temperatures.

The second sampling problem is the asynoptic sampling of the satellites, including the effects of cloud cover that undersamples the diurnal cycle and therefore causes biases with respect to the high frequency synoptic sampling that is possible with GCMs. These biases can be very large for the channels that have a large diurnal cycle (e.g., surface temperature). Because the biases are regionally dependent, it is difficult to remove them from the observations. Meaningful comparisons with GCMs require a sampling strategy that closely resembles the real satellite sampling characteristics.

The most accurate strategy to compare GCM simulated brightness temperatures against TOVS data is that tested with EXACTSAT because simulating the actual satellite orbit at the temporal and spatial resolution of GCMs allows accounting for 1) the drift of the satellite orbit with time; 2) the change in equatorial crossing times between the successive NOAA-series satellites; and 3) the asynoptic sampling of the satellite on the computation of the monthly averaged brightness temperatures. However, the implementation of the EXACTSAT sampling in GCMs is an arduous task. The IDEALSAT experiment yields similar results as EXACTSAT, but is as cumbersome as EXACTSAT to implement, especially for seventeen year climate simulations.

This study demonstrates that, for many applications, GMT sampling of a climate model may be a reasonable approximation if the reference observational data set of brightness temperatures consists of two or more satellites. The sampling biases due to cloud cover are not removed, but the sampling of the diurnal cycle is relatively close to the EXACTSAT sampling. The biases that are introduced are within a few degrees Kelvin and hard to remove with other sampling strategies.

However, if there is only one satellite available, the GMT sampling has large biases. Our introduced LOCALSOL sampling is a much better approximation in this case. It is fairly straightforward to implement in GCM simulations and provides monthly mean brightness temperatures that are close to the exact satellite sampled brightness temperatures. However, the cloud sampling problem remains.

As mentioned above, two error sources will always remain unless we use the exact satellite sampling in the GCM. These are the biases introduced by the extensive cloud cover biasing the satellite data set to cooler morning temperatures, and the unequally spaced satellite overpasses at high latitudes in the Northern Hemisphere biasing the satellite data set to higher day-time brightness temperatures.

In our study biases are the largest for the satellite channels sensitive to surface and lower tropospheric temperatures. It is important to realize, however, that the results of this study are based solely on model calculations. In the real world the diurnal cycles of the brightness temperatures for the different TOVS channels could be different. This is likely to be the case in the upper troposphere where satellite data indicate the presence of a significant diurnal cycle in the water vapor concentrations. Further testing with additional models may prove informative, as well as a closer examination of the treatment of clouds in our approach.

3. Acknowledgements

The work of Richard Engelen was supported by NOAA Grant NA67RJ0152 and NASA Grant NAG5-3449. Laura Fowler's work was supported by NASA Grant NAG-1-1266, NASA Contract NAS1-98125, and DOE Grant DE-FG03-95ER62102. The work by Peter Gleckler and Michael Wehner was performed under the auspices of the Department of Energy Environmental Sciences Division by the Lawrence Livermore National Laboratory under contract W-7405-ENG-48. Graeme L. Stephens and David Randall are thanked for their valuable comments and suggestions.

References

Barkstrom, B.R., The Earth Radiation Budget Experiment (ERBE), Bull. Amer. Meteor. Soc., 65, 1170 - 1185, 1984.

Basist, A.N., and M. Chelliah, Comparison of tropospheric temperatures derived from the NCEP/NCAR reanalysis, NCEP operational analysis, and the microwave sounding unit, Bull. Amer. Meteor. Soc., 78, 1431 - 1447, 1997.

Bates, J.J., X. Wu, and D.L. Jackson, Interannual variability of upper-tropospheric water vapor band brightness temperature, J. Climate, 9, 427 - 438, 1996.

Brooks, D.R., E.F. Harrison, P. Minnis, J.T. Suttles, and R.S. Kandel, Development of algorithms for understanding the temporal and spatial variability of the earth's radiation balance, Rev. Geophys., 24, 422 - 438, 1986.

Cess, R.D., and G.L. Potter, Exploratory studies of cloud radiative forcing with a general circulation model, Tellus Ser. A, 39, 460 - 473, 1987.

Christy, J.R., R.W. Spencer, and E.S. Lobl, Analysis of the merging procedure for the MSU daily temperature time series, J. Climate, 11, 2016 - 2041, 1998.

Ding, P., and D.A. Randall, A cumulus parameterization with multiple cloud base levels, J. Geophys. Res., 103, 11,341 - 11,353, 1998.

Engelen, R.J., and G.L. Stephens, Characterization of water vapour retrievals from infrared TOVS radiances and microwave SSM/T-2 radiances, Quart. J. Roy. Meteor. Soc., 125, 331 - 351, 1999.

Eyre, J.R., On systematic errors in satellite sounding products and their climatological mean values, Quart. J. Roy. Meteor. Soc., 113, 279 - 292, 1987.

Fowler, L.D., and D.A. Randall, Liquid and ice cloud microphysiscs in the CSU general circulation model. Part II: Impact on cloudiness, the Earth's radiation budget, and the general circulation of the atmosphere, J. Climate, 9, 530 - 560, 1996.

Gadgil, S., A. Guruprasad, and J. Srinivasan, Systematic bias in the NOAA outgoing longwave radiation dataset?, J. Climate, 5, 867 - 875, 1992.

Hack, J.J., J.T. Kiehl, and J.W. Hurrell, The hydrologic cycle and thermodynamic characteristics of the NCAR CCM3, J. Climate, 11, 1179 - 1206, 1998.

Hurrell, J.W., and K.E. Trenberth, Difficulties in obtaining reliable temperature trends: reconciling the surface and satellite microwave sounding unit records, J. Climate, 11, 945 - 967, 1998.

Kayano, M.T., V.E. Kousky, and J.E. Janowiak}, Outgoing longwave radiation biases and their impacts on empirical orthogonal function modes of interannual variability in the tropics, J. Geophys. Res., 100, 3173 - 3180, 1995.

McMillin, L.M., and C. Dean, Evaluation of a new operational technique for producing clear radiances, J. Appl. Meteor., 21, 1005 - 1014, 1982.

Mo, K., X.L. Wang, R. Kistler, M. Kanamitsu, and E. Kalnay, Impact of satellite data on the CDAS-reanalysis system, Mon. Weath. Rev., 123, 124 - 139, 1995.

Pan, D.-M., and D.A. Randall, A cumulus parameterization with a prognostic closure, Quart. J. Roy. Meteor. Soc., 124, 949 - 981, 1998.

Randel, D.L., T.H. VonderHaar, M.A. Ringerud, G.L. Stephens, T.J. Greenwald, and C.L. Combs, A new global water vapor dataset, Bull. Amer. Meteor. Soc., 77, 1233 - 1246, 1996.

Rotstayn, L.D., A physically-based scheme for the treatment of stratiform clouds and precipitation in large-scale models. II: Comparison of modelled and observed climatological fields, Quart. J. Roy. Meteor. Soc., 124, 389 - 415, 1998.

Salby, M.L., Climate monitoring from space: asynoptic sampling considerations, J. Climate, 2, 1091 - 1105, 1989.

Salby, M.L., and P. Callaghan, Sampling error in climate properties derived from satellite measurements: consequences of undersampled diurnal variability, J. Climate, 10, 18 - 36, 1997.

Schiffer, R.A., and W.B. Rossow, The International Satellite Cloud Climatology Project (ISCCP): The first project of the World Climate Research Program}, Bull. Amer. Meteor. Soc., 64, 779 - 784, 1983.

Trenberth, K.E., J.R. Christy, and J.W. Hurrell, Monitoring global monthly mean surface temperatures, J. Climate, 5, 1405 - 1423, 1992.

Waliser, D.E., and W. Zhou, Removing satellite equatorial crossing time biases from the OLR and HRC datasets, J. Climate, 10, 2125 - 214, 1997.

Wehner, M., A. Mirin, P. Eltgroth, W. Dannevik, C. Mechoso, J. Farrara, and J. Spahr, Performance of a distributed memory finite difference atmospheric general circulation model, Parallel Computing, 21, 1655 - 1675, 1995.

Wehner, M., and C. Covey, Description and validation of the LLNL/UCLA parallel atmospheric GCM, Tech. Rep. UCRL-ID-123223, Lawrence Livermore National Laboratory, 1995.

Wu, X., J.J. Bates, and S.J.S. Khalsa, A climatology of the water vapor band brightness temperatures from NOAA operational satellites, J. Climate, 6, 1282 - 1300, 1993.

Young, D.F., P. Minnis, D.R. Doelling, G.G. Gibson, and T. Wong, Temporal interpolation for the Clouds and Earth's Radiant Energy System CERES experiment, J. Appl. Meteorol., 37, 572 - 590, 1998.

TABLES

Table 1. Characteristics of TOVS Sounding Channels

Channel number	Central wavenumber	Principal absorbing gases	Average level of maximum contribution	Noise
HIRS 4	704 cm^{-1}	CO_2	400 mb	0.54 K
HIRS 6	732 cm^{-1}	CO_2, H_2O	800 mb	0.54 K
HIRS 8	898 cm^{-1}	Window	Surface	0.80 K
HIRS 10	1217 cm^{-1}	H_2O	900 mb	0.73 K
HIRS 11	1364 cm^{-1}	H_2O	700 mb	0.63 K
HIRS 12	1484 cm^{-1}	H_2O	500 mb	0.85 K
MSU 1	50.31 GHz	Window	Surface	0.54 K
MSU 2	53.73 GHz	O_2	700 mb	0.54 K
MSU 3	54.96 GHz	O_2	300 mb	0.51 K
MSU 4	57.95 GHz	O_2	90 mb	1.30 K

Table 2. Acronyms used to identify sampling strategies

Sampling Method	Acronym
Exact Satellite	EXACTSAT
Ideal Satellite	IDEALSAT
Local Solar Time	LOCALSOL
Exact Model	EXACTMOD
GMT (4/day)	GMT
Monthly Average	MONTHAVG

Table 3. RMS differences (Kelvin) for the LLNL model (January)

Channel	Difference	NOAA 10	NOAA 11	NOAA 10+11
HIRS 8	EXACTSAT - MONTHAVG	3.93	2.64	1.57
	EXACTSAT - EXACTMOD	3.73	2.79	1.39
	EXACTSAT - GMT	3.57	3.09	1.43
	EXACTSAT - LOCALSOL	0.94	2.17	1.06
	EXACTSAT - IDEALSAT	0.57	2.09	1.13
HIRS 12	EXACTSAT - MONTHAVG	1.26	1.32	1.27
	EXACTSAT - EXACTMOD	0.26	0.36	0.24
	EXACTSAT - GMT	0.26	0.36	0.24
	EXACTSAT - LOCALSOL	0.25	0.36	0.24
	EXACTSAT - IDEALSAT	0.26	0.39	0.26

Table 4. RMS differences (Kelvin) for the LLNL model (July)

Channel	Difference	NOAA 10	NOAA 11	NOAA 10+11
HIRS 8	EXACTSAT - MONTHAVG	3.36	2.58	1.69
	EXACTSAT - EXACTMOD	3.05	2.74	1.36
	EXACTSAT - GMT	2.84	3.03	1.38
	EXACTSAT - LOCALSOL	1.81	2.33	1.14
	EXACTSAT - IDEALSAT	0.56	2.34	1.12
HIRS 12	EXACTSAT - MONTHAVG	1.29	1.36	1.30
	EXACTSAT - EXACTMOD	0.32	0.44	0.30
	EXACTSAT - GMT	0.32	0.44	0.30
	EXACTSAT - LOCALSOL	0.32	0.44	0.30
	EXACTSAT - IDEALSAT	0.32	0.45	0.30

Table 5. RMS differences (Kelvin) for the CSU model (January)

Channel	Difference	NOAA 10	NOAA 11	NOAA 10+11
HIRS 8	EXACTSAT - EXACTMOD	1.91	1.69	0.66
	EXACTSAT - GMT	1.98	1.66	0.74
	EXACTSAT - LOCALSOL	0.65	1.24	0.61
	EXACTSAT - IDEALSAT	0.39	1.12	0.66
HIRS 12	EXACTSAT - EXACTMOD	0.35	0.36	0.26
	EXACTSAT - GMT	0.34	0.36	0.25
	EXACTSAT - LOCALSOL	0.30	0.35	0.24
	EXACTSAT - IDEALSAT	0.33	0.37	0.26

FIGURES

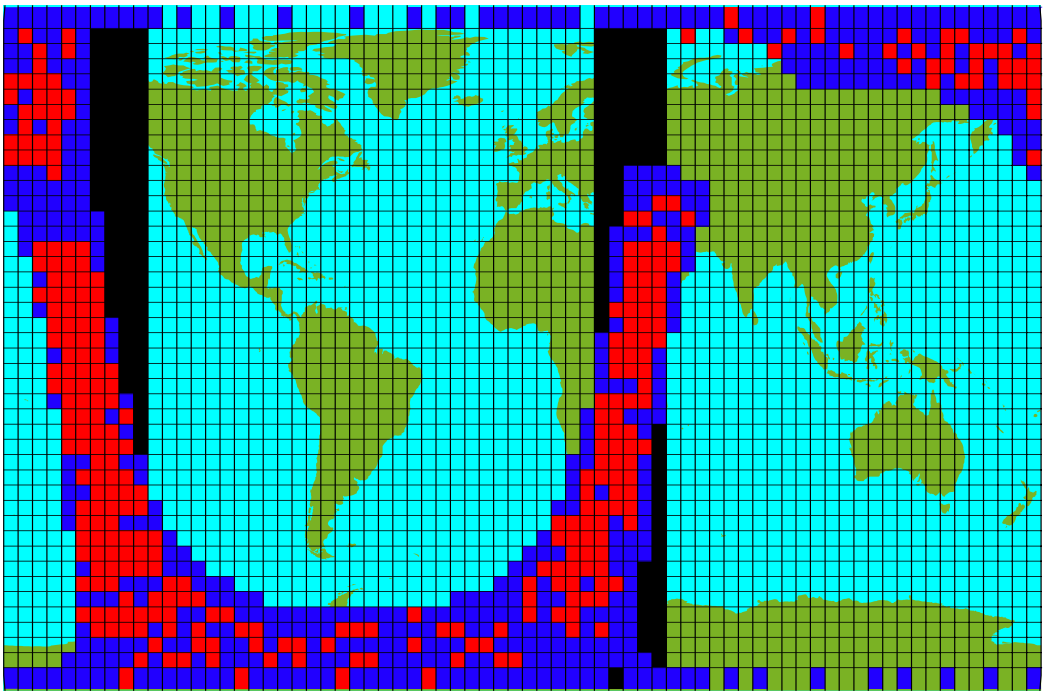

Figure 1. Sampling strategies for the comparison between GCM calculated and TOVS observed brightness temperatures. The grid represents the GCM grid; the black bands represent the local time sampling (LOCALSOL); the blue grid boxes represent the idealized satellite sampling (IDEALSAT); the red grid boxes represent the real satellite sampling (EXACTSAT).

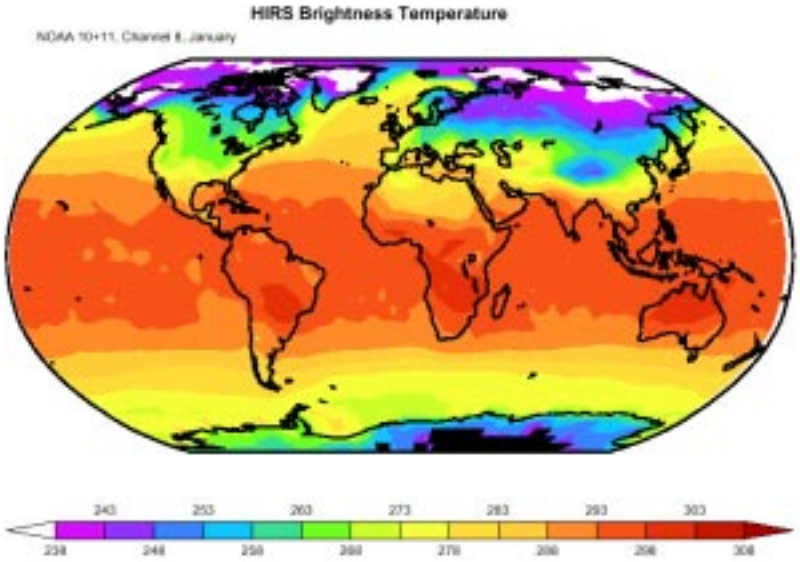

Figure 2. Monthly mean January brightness temperatures in degrees Kelvin for TOVS/HIRS channel 8 using the EXACTSAT sampling.

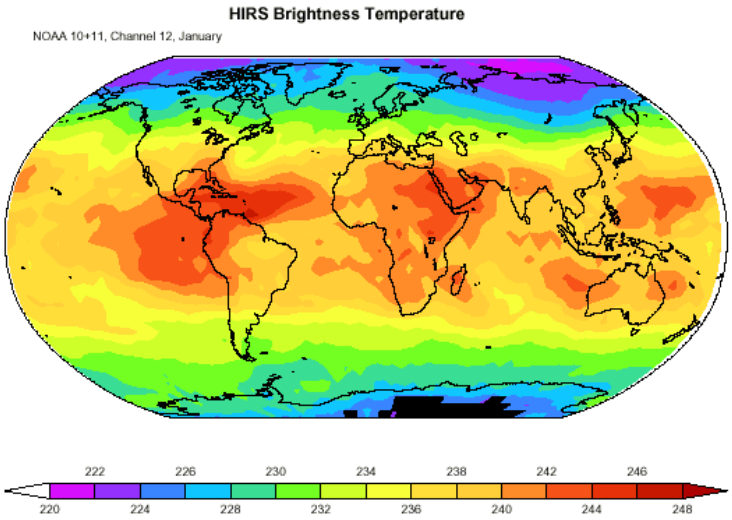

Figure3. Same as Figure 2, but for channel 12.

Fractional Decrease in Number of Satellite Overpasses

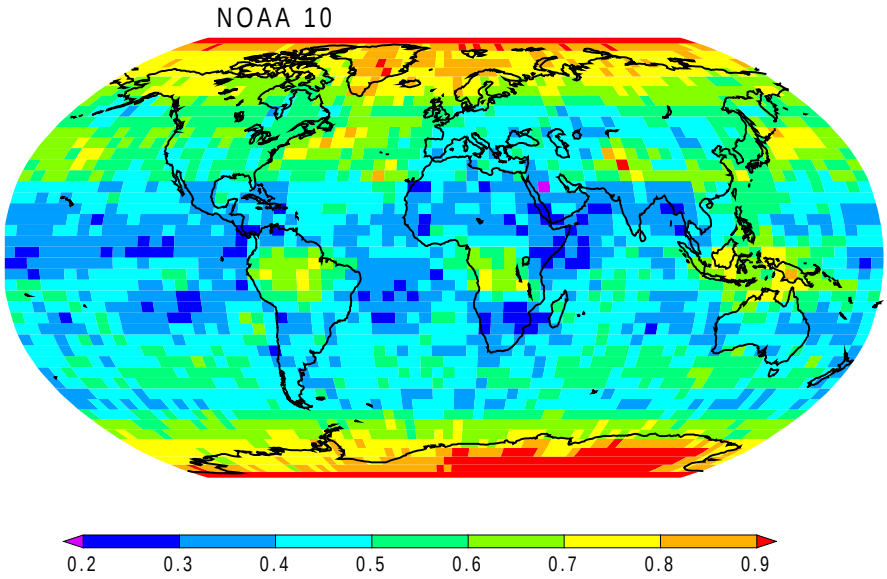

Figure 4. Geographical distribution of the fractional decrease of the number of samples per gridbox going from IDEALSAT to EXACTSAT for NOAA-10.

Fractional Decrease in Number of Satellite Overpasses

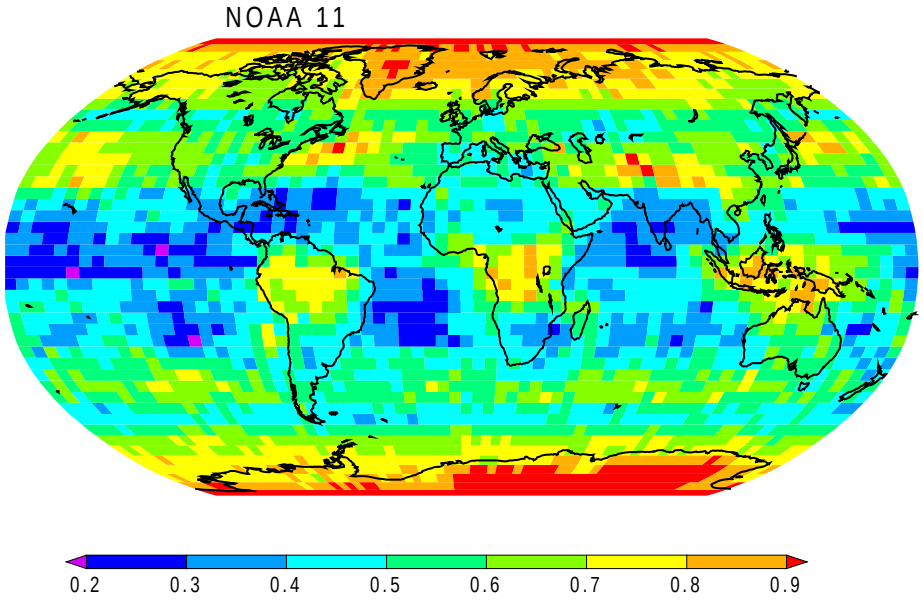

Figure 5. Same as Figure 4, but for NOAA-11.

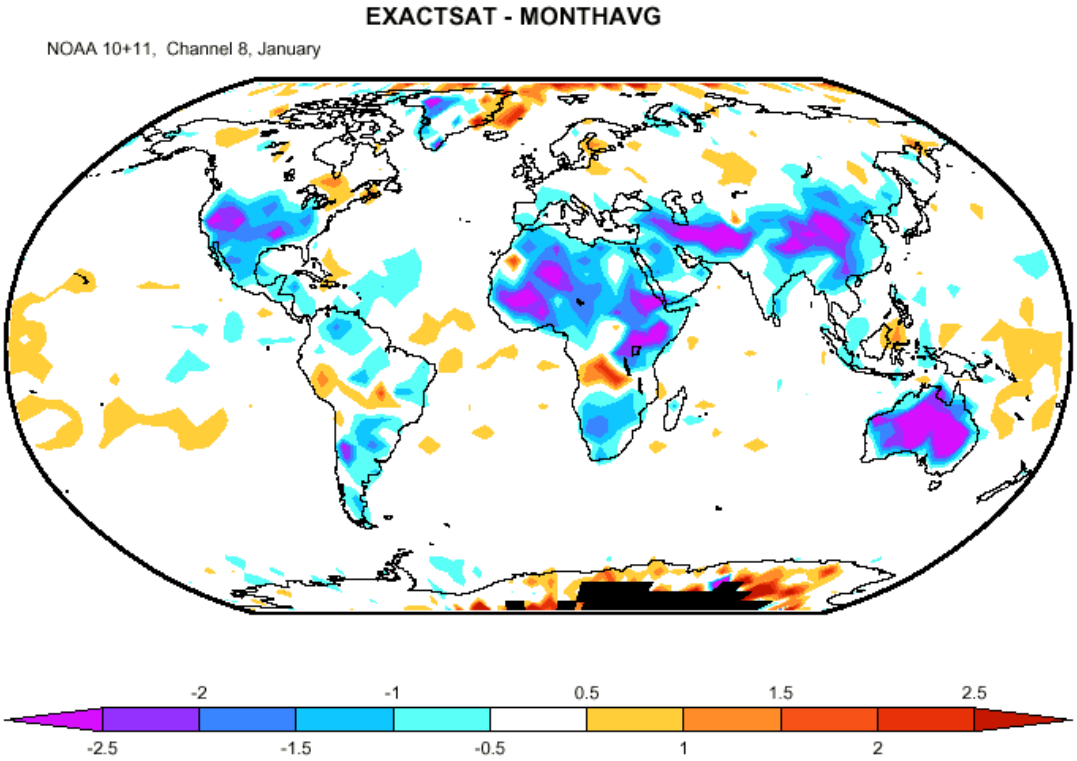

Figure 6. Difference in degrees Kelvin between channel 8 monthly mean brightness temperatures calculated from temperature and water profiles sampled using the EXACTSAT sampling and calculated from monthly mean temperature and water vapor profiles. The results are from the LLNL model.

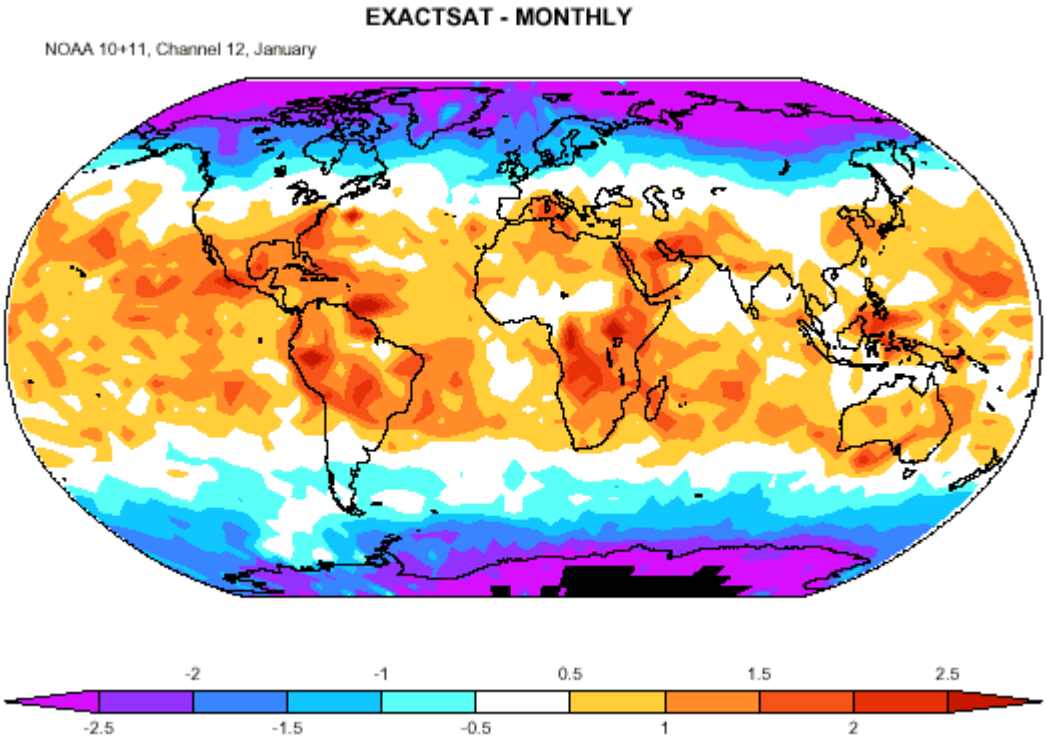

Figure 7. Same as Figure 6, but for channel 12.

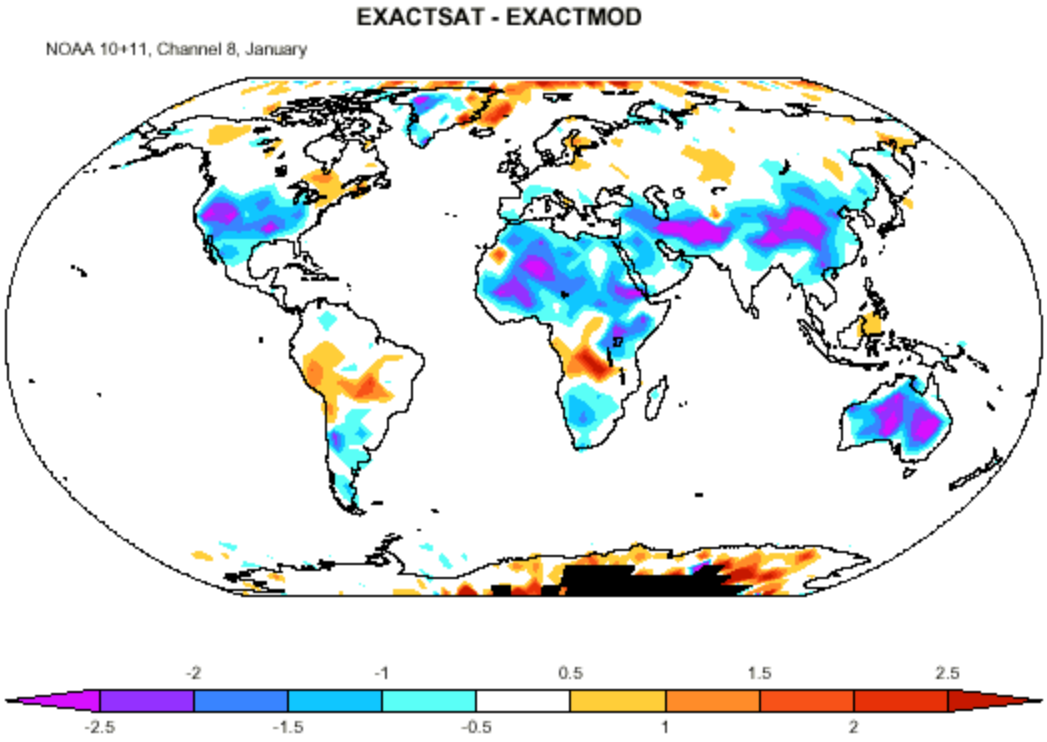

Figure 8. Difference in degrees Kelvin between channel 8 monthly mean brightness temperatures calculated from temperature and water profiles sampled using the EXACTSAT sampling and calculated from hourly sampled mean temperature and water vapor profiles. The results are from the LLNL model.

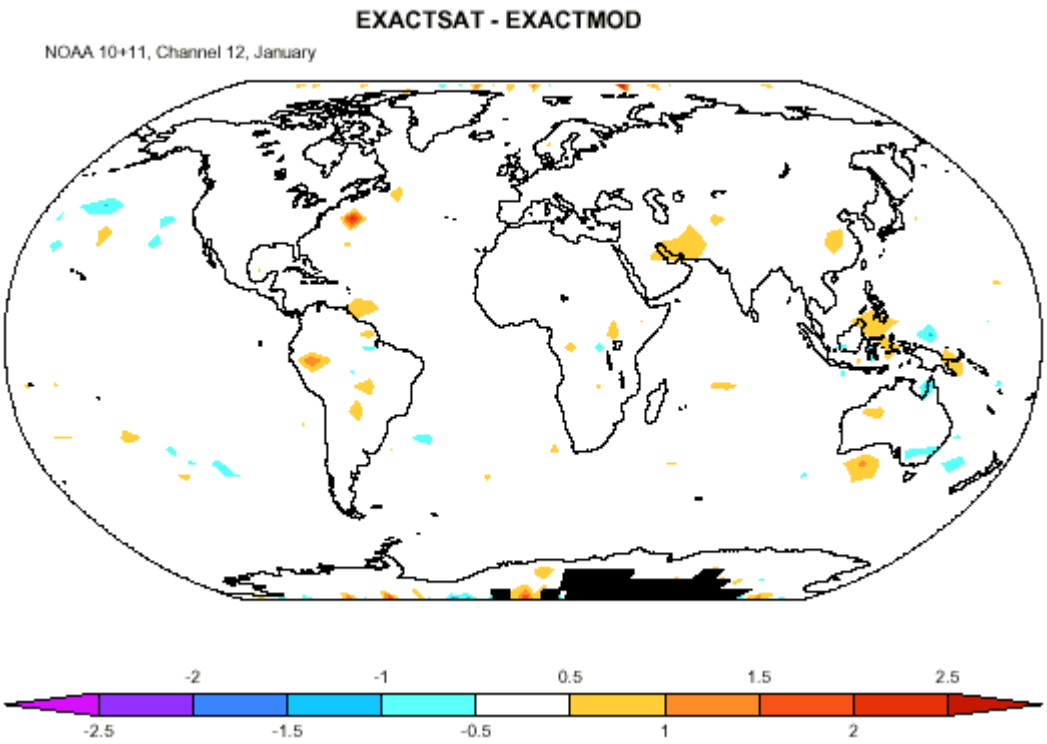

Figure 9. Same as Figure 8, but for channel 12.

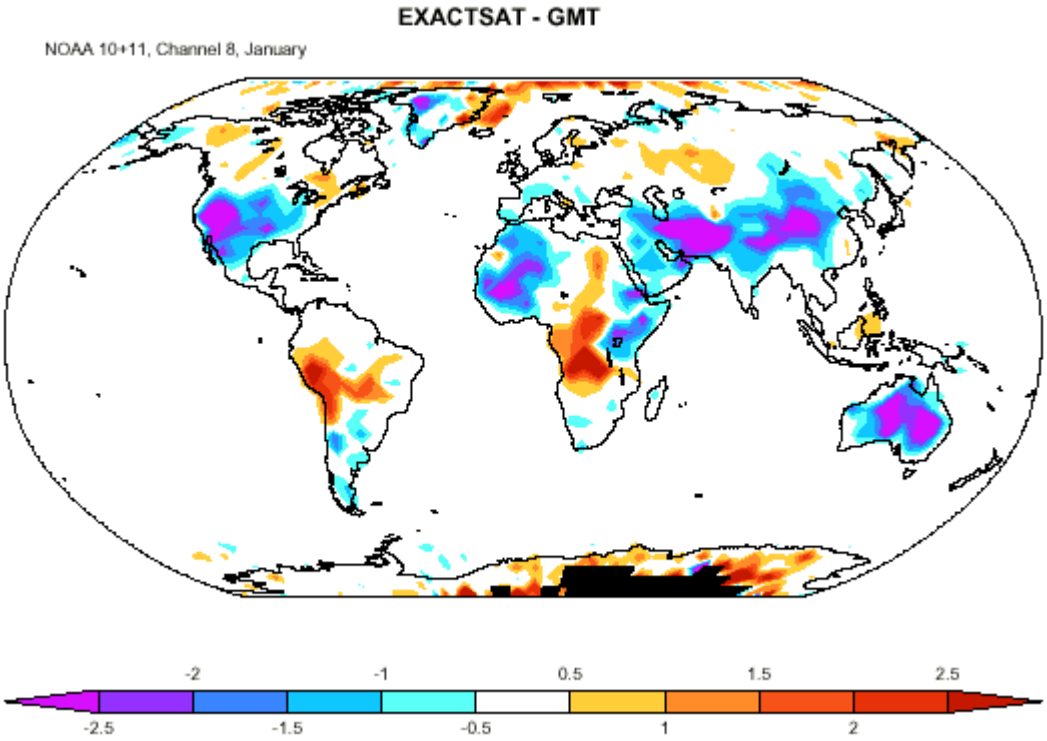

Figure 10. Difference in degrees Kelvin between channel 8 monthly mean brightness temperatures calculated from temperature and water profiles sampled using the EXACTSAT sampling and calculated from temperature and water vapor profiles sampled every 6 hours (GMT). The results are from the LLNL model for January.

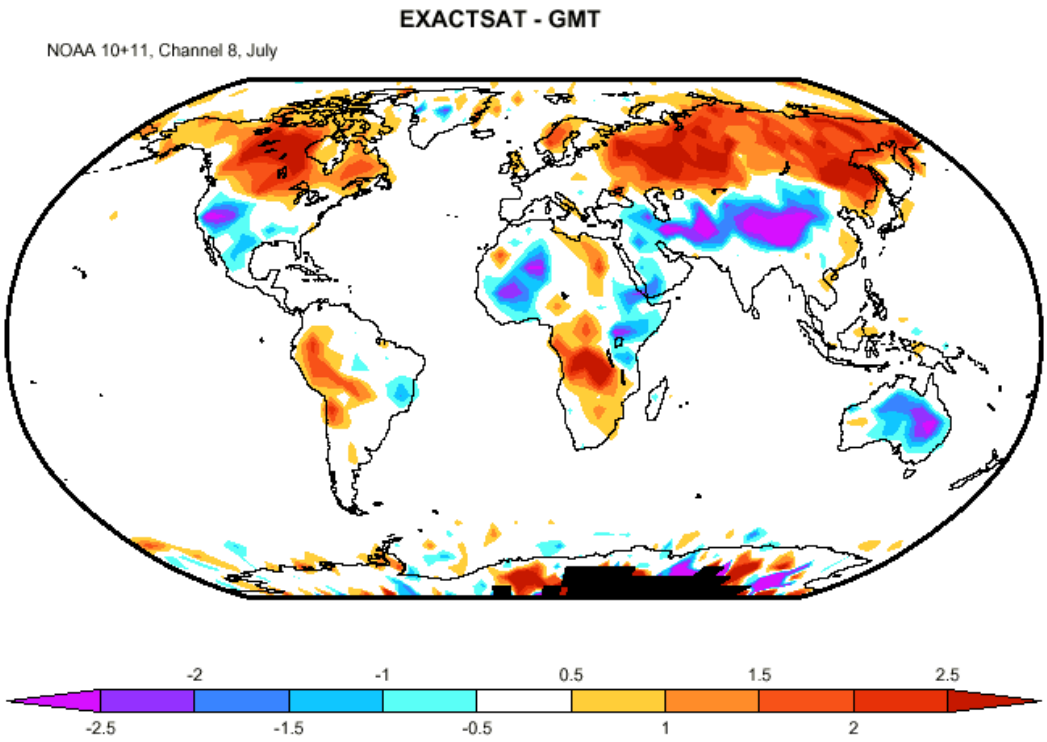

Figure 11. Same as Figure 10, but for July.

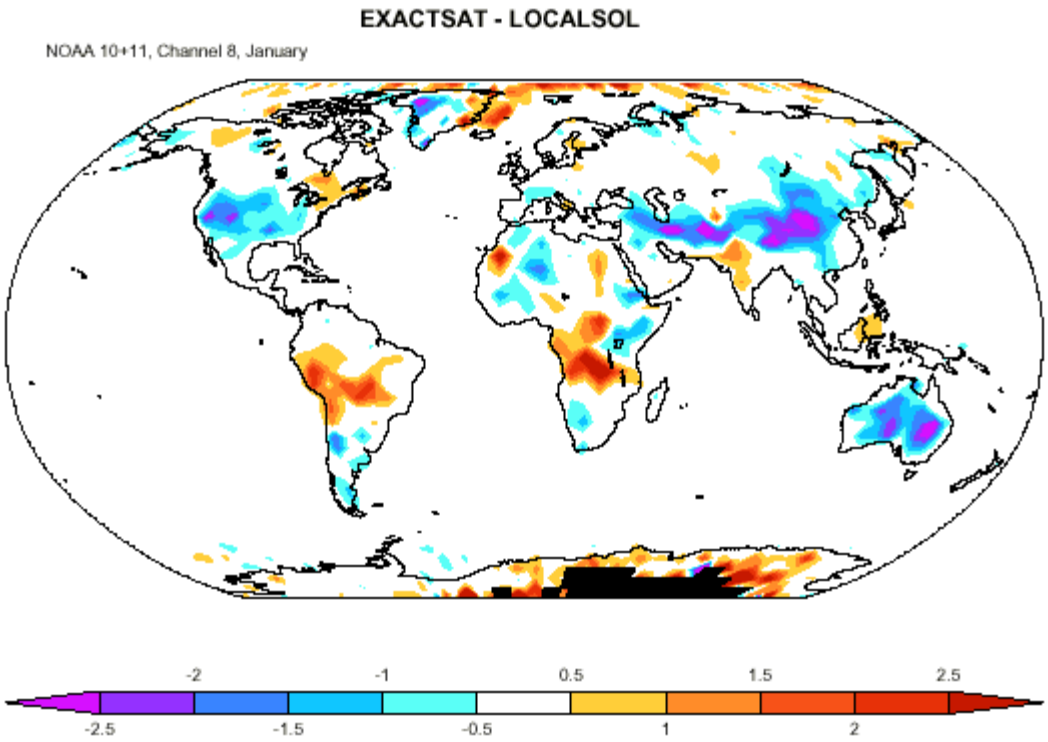

Figure 12. Difference in degrees Kelvin between channel 8 monthly mean brightness temperatures calculated from temperature and water profiles sampled using the EXACTSAT sampling and calculated from temperature and water vapor profiles sampled using the LOCALSOL sampling method. The results are from the LLNL model for January.

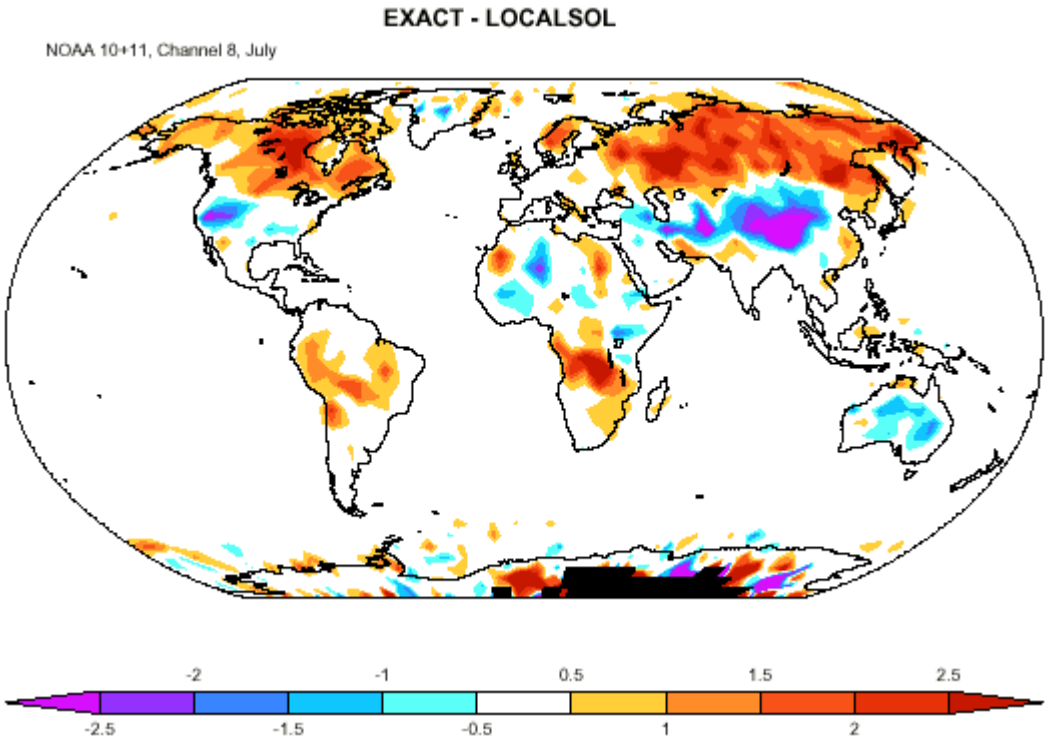

Figure 13. Same as Figure12, but for July.

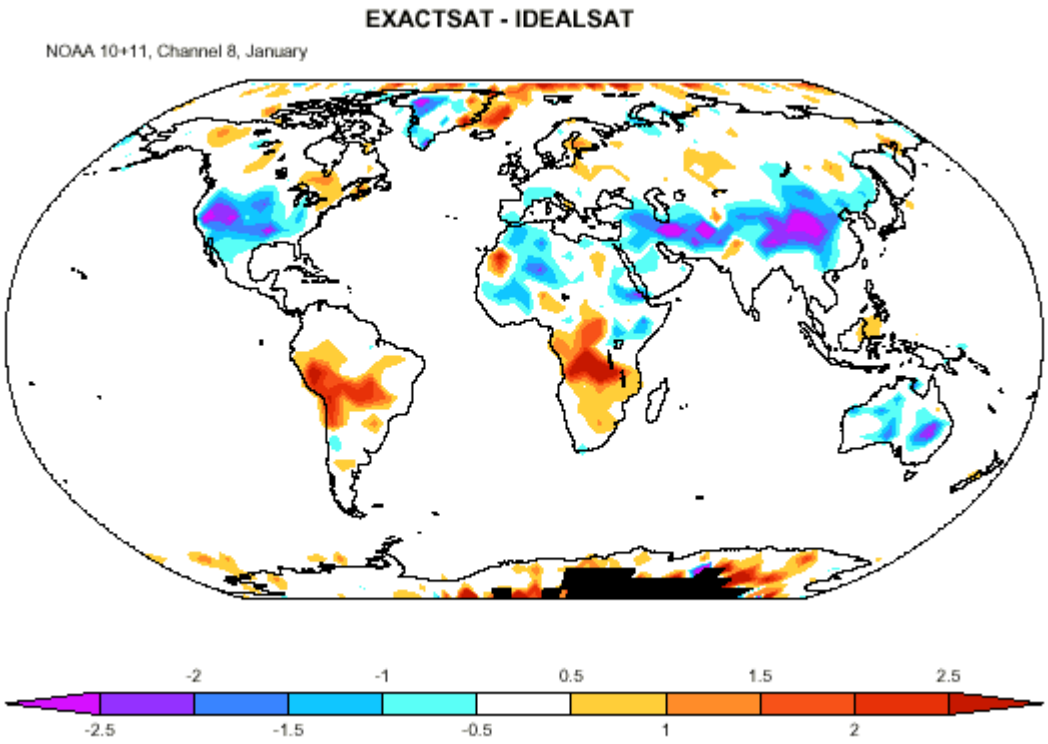

Figure 14. Difference in degrees Kelvin between channel 8 monthly mean brightness temperatures calculated from temperature and water profiles sampled using the EXACTSAT sampling and calculated from temperature and water vapor profiles sampled using the IDEALSAT sampling method. The results are from the LLNL model for January.

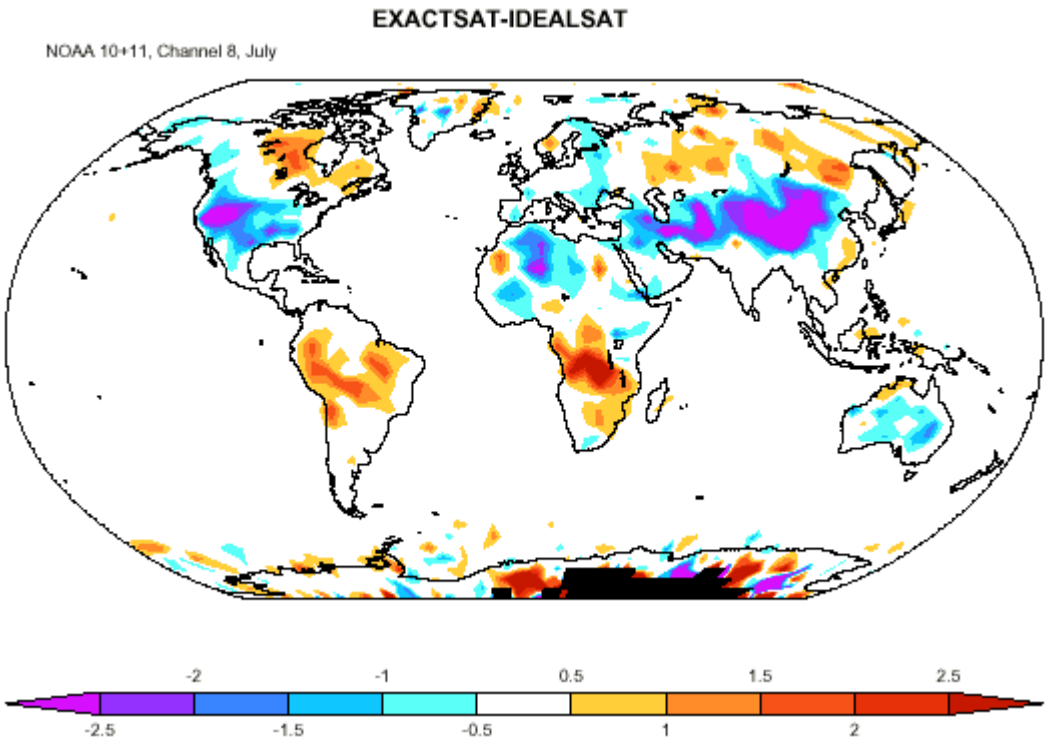

Figure 15. Same as Figure14, but for July.

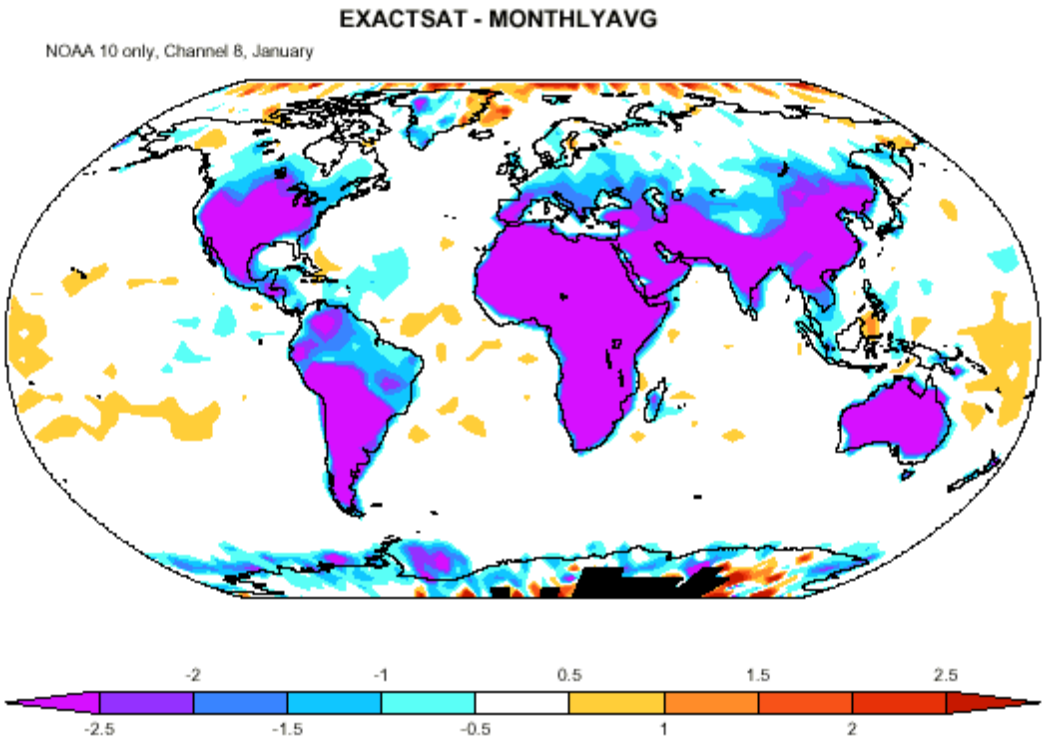

Figure 16. Difference in degrees Kelvin between channel 8 monthly mean brightness temperatures calculated from temperature and water profiles sampled using the EXACTSAT sampling and calculated from monthly mean temperature and water vapor profiles. Only one satellite is used for the EXACTSAT calculations.

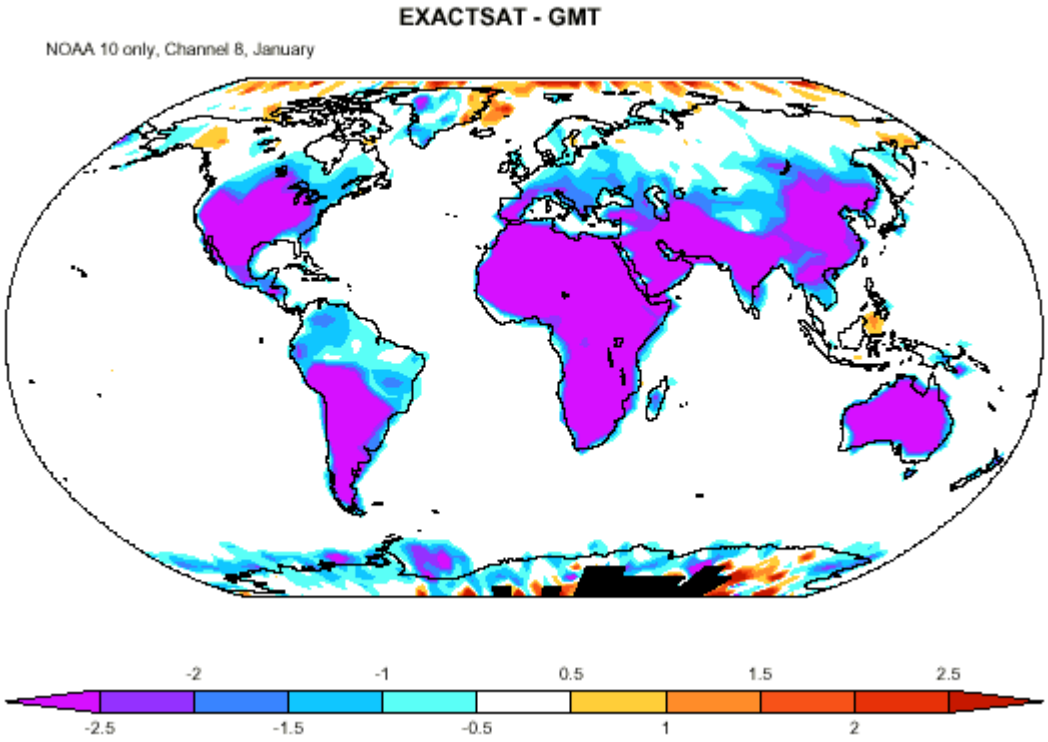

Figure 17. Difference in degrees Kelvin between channel 8 monthly mean brightness temperatures calculated from temperature and water profiles sampled using the EXACTSAT sampling and calculated from temperature and water vapor profiles sampled with the GMT sampling method. Only one satellite is used for the EXACTSAT calculations.

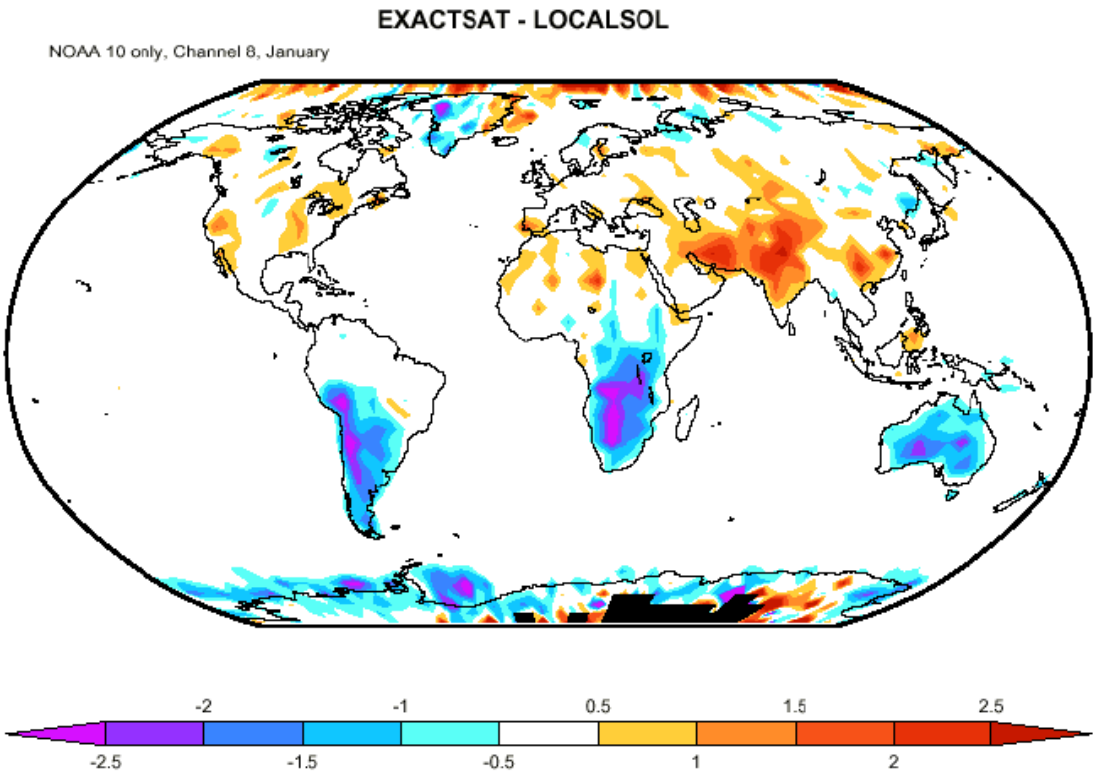

Figure 18. Difference in degrees Kelvin between channel 8 monthly mean brightness temperatures calculated from temperature and water profiles sampled using the EXACTSAT sampling and calculated from temperature and water vapor profiles sampled with the LOCALSOL sampling method. Only one satellite is used for the EXACTSAT calculations.

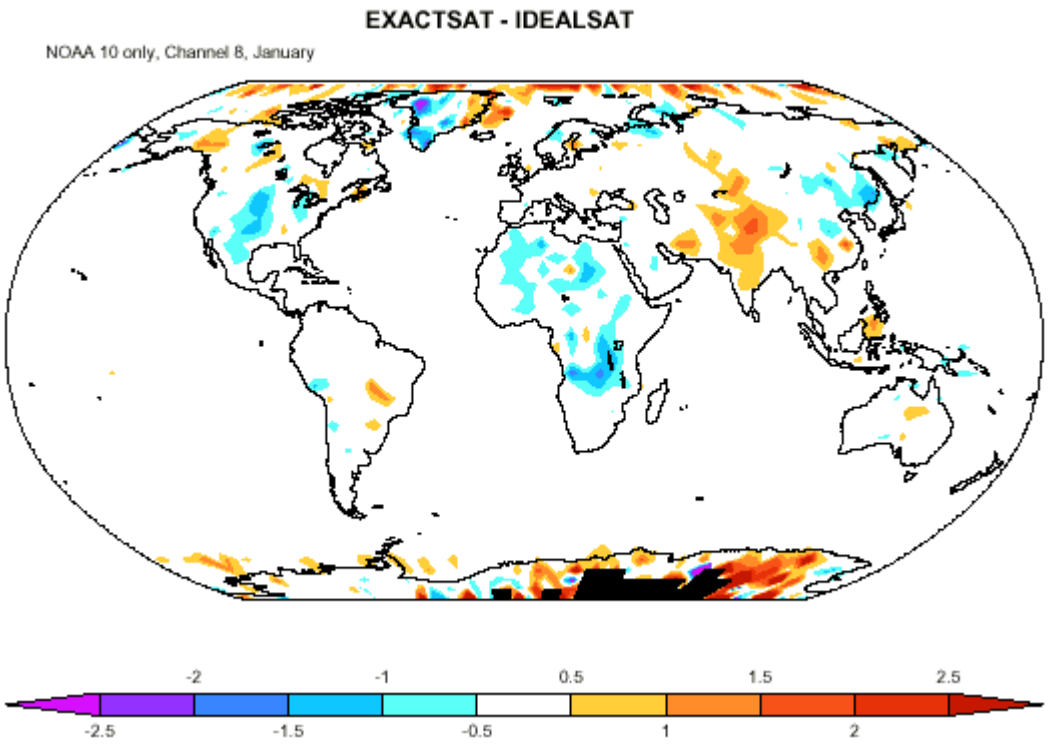

Figure 19. Difference in degrees Kelvin between channel 8 monthly mean brightness temperatures calculated from temperature and water profiles sampled using the EXACTSAT sampling and calculated from temperature and water vapor profiles sampled with the IDEALSAT sampling method. Only one satellite is used for the EXACTSAT calculations.